Journal of Organometallic Chemistry 695 (2010) 2679–2686

Contents lists available at ScienceDirect

Journal of Organometallic Chemistry

journal homepage: www.elsevier.com/locate/jorganchem

Ion pairing in NHC gold(I) olefin complexes: A combined experimental/theoretical study

Nicola Salvi, Leonardo Belpassi, Daniele Zuccaccia, Francesco Tarantelli, Alceo Macchioni*

Dipartimento di Chimica, Università degli Studi di Perugia, Via Elce di Sotto 8, 06123 Perugia, Italy

ARTICLE INFO

Article history:
Received 22 July 2010
Received in revised form
17 August 2010
Accepted 24 August 2010
Available online 1 October 2010

Keywords:
Ion pairing
NOE NMR
DFT
N-heterocyclic carbenes
Gold–alkene complexes

ABSTRACT

The relative anion–cation orientation in [(NHC)Au(alkene)]BF_4 ion pairs [NHC = N-Heterocyclic Carbene = 1,3-bis(di-iso-propylphenyl)-imidazol-2-ylidene (IPr) and 4,5-dimethyl-N,N′-bis(2,6-diiso-propylphenyl)-imidazol-2-ylidene (^{Me}IPr); alkene = 4-methyl-1-pentene, 2,3-methyl-2-butene and 4-methylstyrene] has been investigated by combining $^{19}F,^{1}H$-HOESY NMR spectroscopy in CD_2Cl_2 and a detailed analysis of the Coulomb potential of the cationic fragment through DFT calculations. Two main orientations have been found where the anion locates close to the imidazole ring (*NHC-side*) and close to the olefin (*olefin-side*). The *NHC-side* orientation is always predominant (65–83%) while the exact position of the anion in the *olefin-side* is finely tuned by the nature of olefin substituents. In all cases, the counterion resides far away from the gold site, the latter carrying only a small fraction of the positive charge.

1. Introduction

Au(I) compounds have been increasingly used as catalysts in a large variety of reactions [1] including additions of nucleophiles to alkenes, alkynes, allenes, dienes, and other unsaturated substrates [2]. The key intermediate of such catalytic reactions can be formulated as the ion pair [L–Au–S]X, where L is the ancillary ligand (usually a carbene or a phosphine), S is the substrate to be activated and X^- is a weakly coordinating anion. It is now evident that a proper design of not only L but also the counterion X^- is necessary in order to improve the catalytic activity [3,4], regio-selectivity [5] and even stereo-selectivity [6–8]. A remarkable example of the latter concept has been reported by Toste and co-workers [7a]. By studying the asymmetric hydroalkoxylation of allenes, they found that the utilization of chiral counterions paired with achiral cationic catalysts led to higher *ees* than those obtained with chiral ancillary ligands and achiral counterions [7a].

Despite these well-recognized ion pairing effects [9], the relative anion–cation position(s), that is supposed to be critical in affecting catalytic performances, is often hypothesized basing on rather speculative and indirect arguments, while, in principle, it could be precisely determined basing on interionic NOE (Nuclear Overhauser Effect) NMR measurements [10,11,12,13] possibly integrated with theoretical calculations [14]. This is partially due to the difficulties of isolating the key intermediates of the catalytic processes. Focusing on gold(I) catalysis, the isolation of [L–Au–S]X is not trivial [15] and has been achieved in a few cases using phosphines [16], N-heterocyclic carbenes (NHCs) [17] and cyclic (alkyl)(amino) carbenes (CAACs) [18] as ancillary ligands and alkenes [19] and alkynes [20] as substrates. Only very recently, some preliminary studies on the interionic structure of [L–Au–S]X have been reported [21,22]. They are based on NOE NMR and DFT investigations. The main result is that the gold center is not the preferred acidic-anchor point for the anion, despite its formal +1 charge, and the exact position of the anion is subtly dependent on the nature of L and S.

Since [L–Au–S]X species are known to be rather stable when L = NHC and S = alkenes, we decided to undertake a systematic investigation of the interionic structure of [(NHC)Au(alkene)]X ion pairs (**1**–**4**BF_4, Scheme 1) by combining NOE NMR spectroscopy and quantum chemical calculations [23] based on relativistic Density Functional Theory (DFT) and a detailed analysis of the Coulomb potential of the cationic fragment. The results are reported herein. The main goal of our studies is the understanding of how steric and electronic properties of the NHC-ligand and alkene substrate modulate the ion pair structure. This approach has been successfully applied to investigate Pt(II) [24], Pd(II)[25] and Ru(II)[26] ion pairs, revealing, in some cases, clear relationships between the interionic structure and the chemical reactivity and catalytic performance [27].

* Corresponding author. Tel.: +39 75 5855579; fax: +39 75 5855598.
E-mail address: alceo@unipg.it (A. Macchioni).

0022-328X/$ – see front matter © 2010 Elsevier B.V. All rights reserved.
doi:10.1016/j.jorganchem.2010.08.035

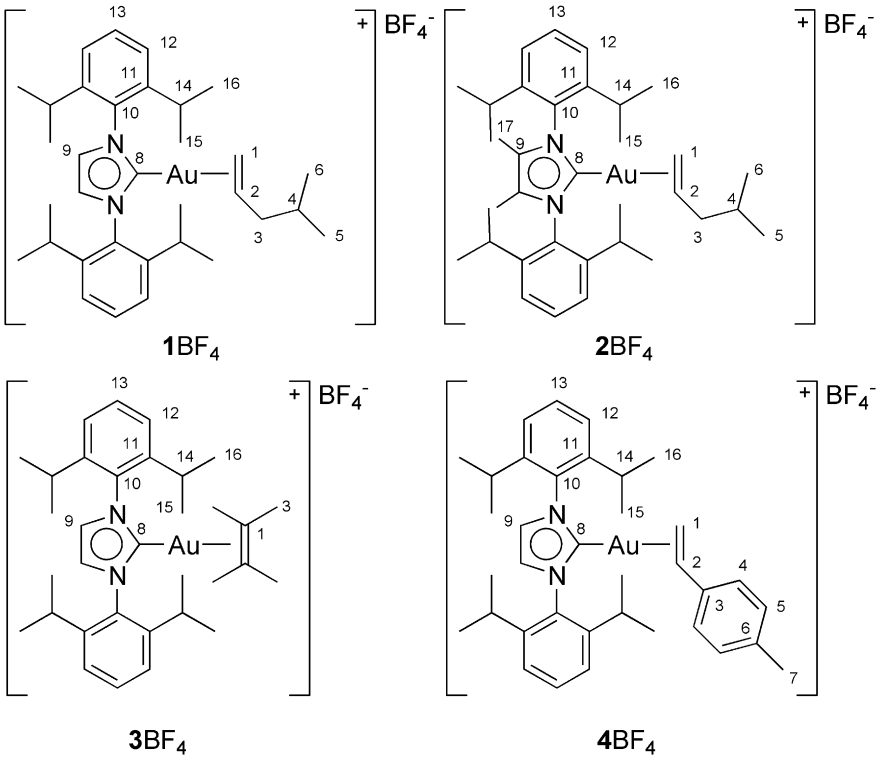

Scheme 1. NHC gold (I) olefin complexes.

2. Results and discussion

2.1. Synthesis and intramolecular characterization of the complexes

Complexes **1**BF_4, **2**BF_4, **3**BF_4 [17b] and **4**BF_4 [22](Scheme 1) have been synthesized by the reaction of $AgBF_4$ with the neutral precursors [(IPr)Au–Cl] [28] (**5**) and [(^{Me}IPr)Au–Cl] [29] (**6**) and the appropriate alkene in CH_2Cl_2. They have been isolated as white powders, after the removal of AgCl from the reaction mixture (Experimental Section).

The assignment of all ^{1}H and ^{13}C NMR resonances of complexes **1**–**4**BF_4, which is preliminary to the investigation of the relative anion–cation orientation in the ion pairs, has been carried out by crossing together the information coming from ^{1}H, ^{13}C, ^{1}H-COSY, ^{1}H-NOESY, ^{1}H, ^{13}C-HMQC, and ^{1}H, ^{13}C-HMBC NMR experiments. Data are reported in the Experimental Section. **1**–**4** cations are particularly suitable to individuate preferential anion locations since they have magnetically inequivalent protons, which can be used as "reporters", well-distributed in almost all the directions of the space. Even the two methyl groups of the isopropyl moieties are inequivalent and can be easily assigned by their selective NOE interactions with olefin and NHC protons (Fig. 1).

Experimental information on the olefin–gold interaction in complexes **1**–**4**BF_4 has been obtained looking at the variation of the ^{1}H [$\Delta\delta^{1H} = \delta^{1H}$(complex) $- \delta^{1H}$(free or precursor)] and, particularly, ^{13}C [$\Delta\delta^{13C} = \delta^{13C}$(complex) $- \delta^{13C}$(free or precursor)] chemical shifts taking free alkene and the starting neutral precursors **5** and **6** as references (Table 1). Olefin coordination causes a deshielding of the imidazol carbons that is more marked for C8 ($\Delta\delta^{13C}$ = 4.2/5.5), directly bounded to gold, than for C9 ($\Delta\delta^{13C}$ about 1.5/2.3) in **1**BF_4, **2**BF_4 and **4**BF_4 complexes. In the case of **3**BF_4 both carbon C8 and C9 are only slightly deshielded by the same value, ca. 1 ppm.

As a consequence of the coordination of the olefin to the metal center, carbons C1 and C2 of **1**BF_4, **2**BF_4 and **4**BF_4 complexes are shielded; the effect is more pronounced for C1 ($\Delta\delta^{13}$C = -19 ppm for **1**BF_4 and **2**BF_4 while $\Delta\delta^{13}$C = −28 ppm for **4**BF_4) than for C2 ($\Delta\delta^{13}$C = −4.8, −6.1 and −9 ppm for **1**BF_4, **2**BF_4 and **4**BF_4 respectively) indicating an unsymmetrical coordination of the double bond with carbon C1 closer to the metal center [30]. In the case of **3**BF_4 carbon C1 is only marginally shielded by about 1 ppm. The observed shifts are consistent with those reported in the literature [17b,17e].

In order to investigate in greater detail the structural aspects and the electronic structure of the complexes, we have carried out DFT calculations on **1**$^+$, **2**$^+$, **3**$^+$ and **4**$^+$, performing geometry optimizations in CH_2Cl_2 solution (see Experimental Section for technical details). The principal geometrical parameters obtained for these complexes are reported in Table 2. The complete set of optimized coordinates for our complexes are given in the Supplementary information.

The data show, first of all, that the bond distance between Au and C8 is nearly constant (about 2.05 Å) along the series **1**$^+$–**4**$^+$, remaining essentially unaffected either by methyl substitution at position 9 of the carbene ring (compare, e.g., **1**$^+$ and **2**$^+$) or by substitutions at the alkene (**1**$^+$ and **3**$^+$). More significant geometrical modifications are found in the alkene moiety itself. In complex **1**$^+$, the 4-methyl-1-pentene double bond C1–C2 is longer by about 0.04 Å than in the free system. The dihedral angle H1trans–C1–C2–C3 is reduced from 180° to 159° upon coordination, while H1cis–C1–C2–2 presents a smaller distortion (10°). In particular, our DFT calculations show the Au–C1 distance (2.27 Å) to be significantly shorter (by 0.13 Å) than Au–C2 (2.40 Å), confirming the unsymmetrical coordination of 4-methyl-1-pentene to the gold (I) site. This is consistent also with X-ray structures of similar complexes [17b]. For example, in [(NHC)Au(H_2C=CMe_2)]SbF_6 (**1a** in Table 2) the distance of the disubstituted carbon C2 from gold is about 0.09 Å longer than the Au–C1 distance.

The introduction of two methyl groups in position 9, leading from complex **1**$^+$ to complex **2**$^+$, affects almost negligibly the

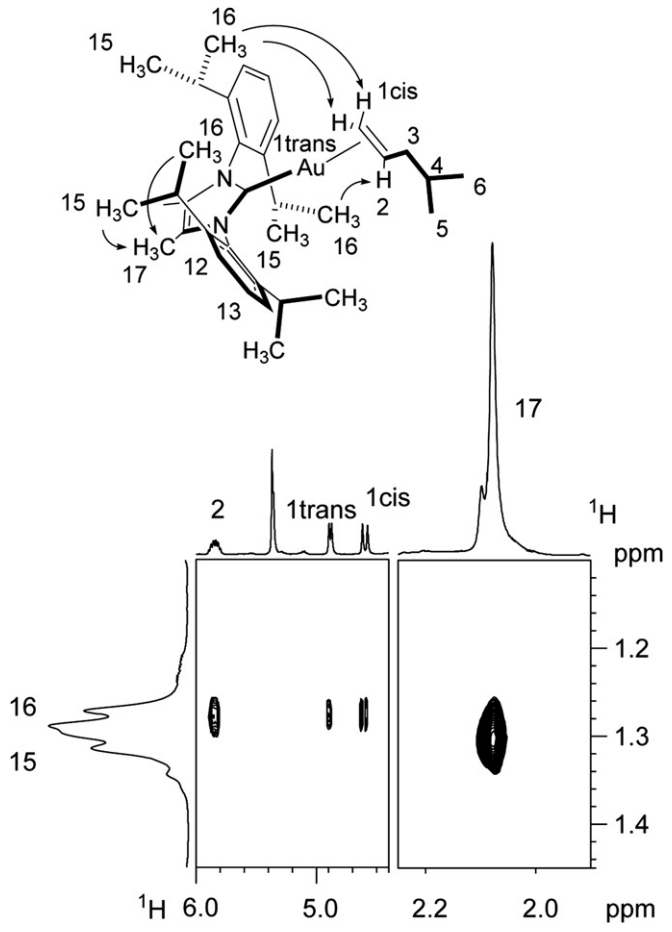

Fig. 1. A section of the ^{1}H-NOESY NMR spectrum (400.13 MHz, 298 K, CD_2Cl_2) of the complex **2**BF_4.

coordination geometry of the alkene substrate, in particular for what concerns the pronounced asymmetry of double bond coordination and the distortion of its dihedral angles. In complex $\mathbf{3}^+$, the coordinated 2,3-methyl-2-butene has a double bond again slightly longer (by about 0.05 Å) than the free alkene, system, an elongation quite close to that found for the complexes $\mathbf{1}^+$ and $\mathbf{2}^+$. As expected, however, in this case the double bond coordinates symmetrically to gold(I), with a Au–C distance intermediate between the values found for the unsymmetric alkene. The dihedral angles are also distorted symmetrically, by about 20° from the planarity of the free molecule. For complex $\mathbf{3}^+$, X-ray structures are available [17b] and confirm the symmetric coordination. Comparison with our DFT results in solution shows that the latter yield bond distances systematically longer than experiment, with the largest deviation (about 0.1 Å) found for Au–C2. As mentioned above, the available

Table 2
Computed representative geometrical parameters for $\mathbf{1}^+$, $\mathbf{2}^+$, $\mathbf{3}^+$ and $\mathbf{4}^+$.

	Au–C8	Au–C1	Au–C2	C1–C2	C2–Au–C1	H1–C1–C2–X2
$\mathbf{1}^+$	2.054	2.272	2.401	1.380 (1.339)	34.2	159 (*H*1 = 1trans X2 = C3) 170 (*H*1 = 1cis × 2 = H2)
$\mathbf{2}^+$	2.057	2.280	2.399	1.379 (1.339)	34.2	159 (*H*1 = 1trans X2 = C3) 170 (*H*1 = 1cis × 2 = H2)
$\mathbf{3}^+$	2.053	2.346	2.345	1.402 (1.356)	34.8	160
$\mathbf{4}^+$	2.05	2.25	2.42	1.39 (1.34)	34.4	163 (*H*1 = 1trans X2 = C3) 168 (*H*1 = 1cis × 2 = H2)

Distances are in angstrom and angles in degrees. The corresponding computed C1–C2 distances of the free alkenes in solution (CH_2Cl_2) are reported in brackets

computed and experimental data show that the Au–C8 bond distance is remarkably stable with respect to different substitutions in the alkene substrate. Both theoretical calculations and X-ray data suggest that the asymmetrical disubstituted alkenes tend to coordinate gold(I) also unsymmetrically, with the less substituted carbon closer to the metal center. In the cation $\mathbf{4}^+$, where NHC–Au^+ coordinates 4-methylstyrene, the difference between the Au–C2 and Au–C1 distances is 0.17 Å, the largest among the systems considered here.

A detailed analysis of the charge distribution in cations $\mathbf{1}^+$–$\mathbf{4}^+$ has been carried out using the Hirshfeld charge analysis and Voronoi Deformation Density (VDD) and the results are reported in Table 3.

They clearly indicate that the positive charge, formally on the Au(I) site, is significantly redistributed on the ligands. The gold atom actually carries a positive charge not larger than 0.17 and 0.26 electrons in the VDD and Hirshfeld results, respectively, and this value is remarkably invariant for all complexes. The charge associated with C8 is extremely small in both the VDD and Hirshfeld pictures and also does not show meaningful variations along the series. This further confirms that the NHC–Au bond is largely unaffected by methyl substitution at the imidazolium ring. The two charge analysis methods give almost coincident results for the charges at the double bond sites. Unsymmetric coordination of the olefin is seen to be accompanied by an accumulation of the electronic density on the unsaturated carbon atom closer to the metal center (C1) and this charge asymmetry is slightly more pronounced for the more asymmetric bond in $\mathbf{4}^+$. The slightly more pronounced electron accumulation at the C1 site, compared with C2, is entirely consistent with the observed larger ^{13}C NMR shielding (Table 1). It is important to note that the Au–C distance is a crucial factor for the modulation of the nature of the bond in this type of gold(I)–alkene (alkyne) complexes [31]. In particular, the metal-to-substrate π-back-donation component of the Dewar–Chatt–Duncanson model is most sensitive to the substrate distortion and its distance from gold(I). If and how unsymmetric coordination further tunes the character of the Au–C bond, the chemical activity of the two unsaturated carbon atoms is of key interest in catalysis and is currently under investigation in our laboratory.

Table 1
Selected ^{1}H and ^{13}C chemical shift data for complexes **1**BF_4–**4**BF_4.

	C1	H1	C2	H2	C8	C9
1BF_4	96.7(−18.9)	4.95(−0.03) trans 4.66(−0.38) cis	133.8(−4.8)	5.36(−0.45)	180.8(5.2)	125.4(1.7)
2BF_4	96.3(−19.3)	4.88(−0.10) trans 4.59(−0.45) cis	132.5(−6.1)	5.84(0.03)	177.2(5.5)	128.8(2.3)
3BF_4			122.1(−1.6)		176.3(0.7)	124.4(0.7)
4BF_4	84.7(−28.4)	4.91(−0.33) trans 5.02(−0.76) cis	129.4(−9.0)	6.56(−0.18)	179.8(4.2)	125.2(1.5)

$\Delta\delta$ values defined as δ (complex) − δ (free or precursor) is reported in brackets.

Table 3
Charge analysis for $\mathbf{1}^+$, $\mathbf{2}^+$, $\mathbf{3}^+$, $\mathbf{4}^+$ using two different methods: Hirshfeld (Hirsh) and Voronoi Deformation Density (VDD).

	Method	$\mathbf{1}^+$	$\mathbf{2}^+$	$\mathbf{3}^+$	$\mathbf{4}^+$
C8	Hirsh	0.01	0.01	0.02	0.02
	VDD	−0.05	−0.05	−0.04	−0.05
Au	Hirsh	0.26	0.26	0.26	0.26
	VDD	0.17	0.17	0.17	0.17
C1	Hirsh	−0.07	−0.07	0.03	−0.08
	VDD	−0.08	−0.08	−0.02	−0.09
C2	Hirsh	0.01	0.01	0.02	0.00
	VDD	−0.01	−0.01	−0.02	−0.00

2.2. NMR and DFT interionic characterization of complexes

The relative anion–cation orientation in solution of **1**BF_4, **2**BF_4, **3**BF_4 and **4**BF_4 complexes has been investigated by $^{19}F,^1H$-HOESY NMR spectroscopy (Figs. 2, 4 and 6). The detected interionic dipolar NOE interactions are consistent with having in solution two relative anion–cation orientations with BF_4^- locating either at the *NHC-side* or at the *olefin-side*. Such orientations have been previously observed in Ir(III) [32] and Ag(I) [33] NHC complexes (*NHC-side*) and Pt(II) [24] and Pd(II) [25,27] complexes (*olefin-side*). In the present case, their predominance has been rationalized, based on the analysis of the Coulomb potential of the cationic fragments, a property of the molecular systems, the analysis of which has been helpful in a number of investigations [21,22,34]. We mapped the Coulomb potential on an electronic isodensity surface (0.007 e/Å^3). This surface roughly visualizes the steric dimension of the ions [21] (Figs. 3, 5 and 7).

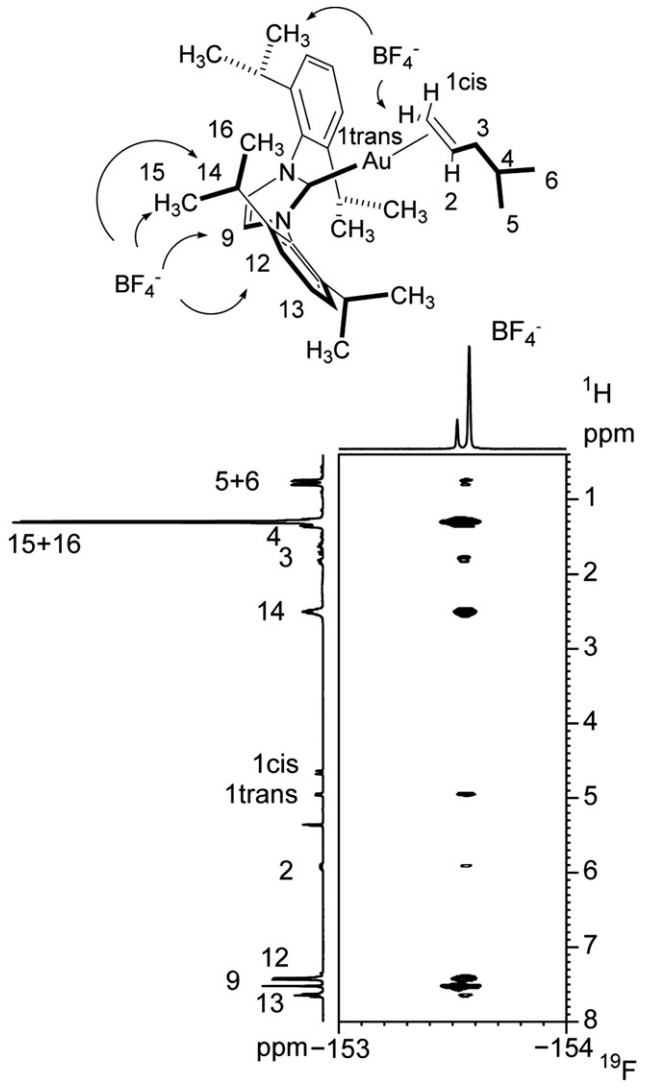

Fig. 2. $^{19}F,^1H$-HOESY NMR spectrum (376.65 MHz, 298 K, CD_2Cl_2) of complex **1**BF_4.

The relative abundance of two orientations has been determined by a quantitative analysis of the interionic NOE intensities, carried out taking into account that the volumes of the cross peaks are proportional to $(n_I n_S/n_I + n_S)$ where n_I and n_S are the number of equivalent I and S nuclei, respectively (Table 4) [35].

Assuming that the minimum distance between the anion and the cation is the same in both the orientations, the abundances have been estimated by the normalized NHC/anion and olefin/anion NOE intensities. H9 and H17 have been chosen as the probes of the *NHC-side* orientation for the **1**BF_4, **3**BF_4, **4**BF_4 and **2**BF_4 ion pairs, respectively. As for the *olefin-side* orientation the protons showing the largest NOEs have been selected as the probes instead of the sum of the intensities in the assumption that a single anion orientation is present on the side of the olefin.

In the $^{19}F,^1H$-HOESY NMR spectrum of complex **1**BF_4 (Fig. 2) strong contacts were detected between the F-atoms of the counterion and H9 of the NHC-ligand. Medium-strength contacts were observed with H12, H14, H15, H16. Weak contacts were present with H1trans, H2, H3, H5 and H6 of the olefin and H13 of the ligand. It is important to note that there was no contact between the F-atoms and H1cis. The intensity ratio of the $BF_4^-\cdots$H9 and $BF_4^-\cdots$H1trans NOEs is 1/0.21 (Table 4) leading to an abundance of the *NHC-side* and *olefin-side* equal to 83% (1/1.21·100) and 17% (0.21/1.21·100), respectively. Consistently with these observations, the H9 sites have the most positive Coulomb potential (Fig. 3) while H1cis, H1trans and H2 are the most electropositive protons of the olefinic fragment.

2BF_4 differs from **1**BF_4 for having two methyl groups in position 9 of the imidazole ring. In $^{19}F-^1H$-HOESY spectrum of **2**BF_4 (Fig. 4), strong contacts are present between the F-atoms of the counterion and H14, H15, H16, H17. Medium-strength contacts were observed with hydrogen 12. Weak contacts were detected with H1trans, H2, H5, H6 and H13. The interaction of H1cis with the counterion is missing also in this case. The most intense NOE is between the anion and H17. However, in this case the intensity of the NOE with H1trans is ca. half of that with H17 (Table 4). As a consequence, the abundance of the *olefin-side* orientation is about 35%. The Coulomb potential of $\mathbf{2}^+$ (Fig. 5) clearly shows that, although H17 is less positively charged than H9 in $\mathbf{1}^+$, the presence of six protons (H17) creates a wide zone of less positive potential in which the anion can be easily trapped (Fig. 5). The consequence is that the anion prefers the *NHC-side* also in **2**BF_4, albeit with a lower selectivity than in **1**BF_4 (65% *versus* 83%).

In the case of **3**BF_4 (Fig. 6 and Table 4), bearing the symmetrical "completely methylated" olefin, a somewhat enhanced specificity toward the *NHC-side* might have been expected, since the most positively H1 and H2 olefinic protons are no longer present. This was not the case. Only one strong contact between the F-atoms of the counterion and H9 was observed. Medium-size contacts were observed with H2, H15 and H16, and small contacts between F-atoms of the counterion and H12, H13 and H14 of the NHC. The most abundant orientation is again the *NHC-side* with a percentage identical to that of **1**BF_4 (83%). The Coulomb potential (Fig. 7) shows that the methyl groups bound to the double bond are less positive than H1 or H2 in **1**–**2**BF_4 but they are still a little positively charged and they offer a more extended area for anchoring the anion. As a result, in **3**BF_4, exactly as in **1**BF_4, there is still a 17% of ion pairs having the anion in the *olefin-side*.

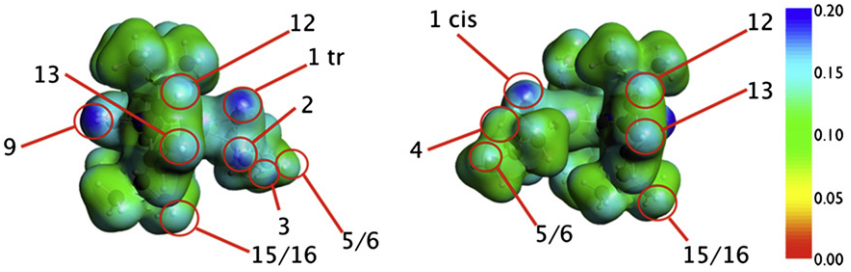

Fig. 3. Two views of the Coulomb potential of 1^+ mapped on an electronic isodensity surface ($\rho = 0.007$ e/Å^3, Coulomb potential in a.u.).

Complex **4**BF_4 has been previously investigated by us, at low temperature, in order to compare its interionic structure with that of an analogous phosphine complex [21]. In the course of the present work, we recorded a $^{19}F,^1H$-HOESY spectrum of **4**BF_4 at room temperature under the same conditions as those for **1**–**3**BF_4. A strong contact between the F-atoms of the counterion and H9 of the NHC-ligand was observed; contacts of medium intensity were detected with H14, H15, H16, H1cis, H1trans, H2 and H4 (Table 4). The relative abundances *NHC-side*/*olefin-side* are 79%/21%, similar to those found in **1**BF_4 and **3**BF_4. A close inspection of the NOE intensities of olefinic protons reveals a tiny but significant difference in the anion location within the *olefin-side* orientation in the **1**BF_4 and **4**BF_4 ion pairs. In the former the anion stays closer to the olefinic CH_2 while in the latter it shifts toward H2 approaching the aryl substituent of the olefin. This could be due to the enhanced acidity of H2 caused by the electron-withdrawing nature of the aryl substituent and to the presence of more slightly positive neighbor protons (H4 an H5) in **4**BF_4. Consistently with these findings, the Coulomb potential map of $\mathbf{4}^+$ [21] shows, in addition to the highest positive charge accumulation on H9 [21], positive charge on H1cis, H1trans, H2 but also on H4 and H5 of the phenyl ring.

A common feature of the Coulomb potential of cation $\mathbf{1}^+$–$\mathbf{4}^+$ is the marginal accumulation of positive charge in the region of the gold center (Figs. 3, 5 and 7), as previously observed in phosphine gold(I) compounds [21].

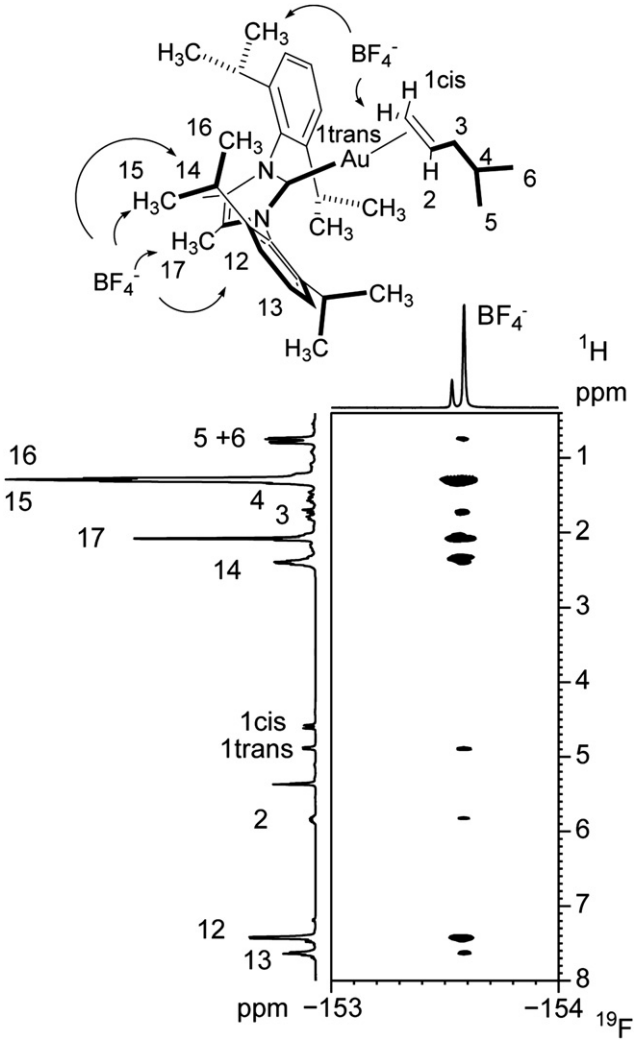

Fig. 4. $^{19}F,^1H$-HOESY NMR spectrum (376.65 MHz, 298 K, CD_2Cl_2) of complex **2**BF_4.

3. Conclusions

In conclusion, we have shown that the combination of experimental results coming from interionic NOE NMR studies and theoretical DFT calculations of the Coulomb potential, provides a reliable methodology for disclosing the relative orientation of the anion and cation within an ion pair. We have applied such a methodology to the investigation of NHC–gold complexes **1**–**4**BF_4 differing in the nature of the carbenes (IPr *versus* ^{Me}IPr) and olefin (4-methyl-1-pentene, 2,3-methyl-2-butene and 4-methylstyrene). Two main orientations have been observed: *NHC-side* and *olefin-side*. The former was always predominant (65–83%). It was found that the substitution of the rather acidic H9 protons of the NHC with methyl groups caused a decrease of the abundance of the *NHC-side* orientation from 83% to 65%. On the contrary, the nature of the olefin little affected the relative abundances of the two orientations but it caused a little shift of the anion toward C2 in the case of 4-methylstyrene. It is remarkable that such effects deriving from differences in energy smaller than 1 kcal/mol could be clearly detected by NMR and completely rationalized with the help of DFT calculations.

4. Experimental section

4.1. Synthesis and NMR intramolecular characterization

$HAuCl_4$, tetrahydrothiophene (THT), glyoxal (40 wt% solution in water), 2,6-diisopropylaniline, HCl in diethyl ether, $AgBF_4$, 4-methylstyrene, 4-methyl-1-pentene and 2,3-methyl-2-butene were purchased from Ricci Chimica and Sigma Aldrich. 4-Methylstyrene was charged in a Schlenk flask and stored in nitrogen atmosphere at −20 °C under activated molecular sieves. $AgBF_4$ was charged in Schlenk flask and stored in nitrogen atmosphere at −20 °C.

The synthesis of compounds 1,3-bis(diisopropylphenyl)imidazolium chloride [36], 4,5-dimethyl-N,N′-bis(2,6-diisopropylphenyl) imidazolium chloride [29], (THT)AuCl [37], [1,3-bis(diisopropylphenyl)imidazol-2-ylidene]Au–Cl [28], [4,5-dimethyl-N,N′-bis(2,6-diisopropyl-phenyl)-imidazol-2-ylidene]Au–Cl [29] were performed according to the literature procedures.

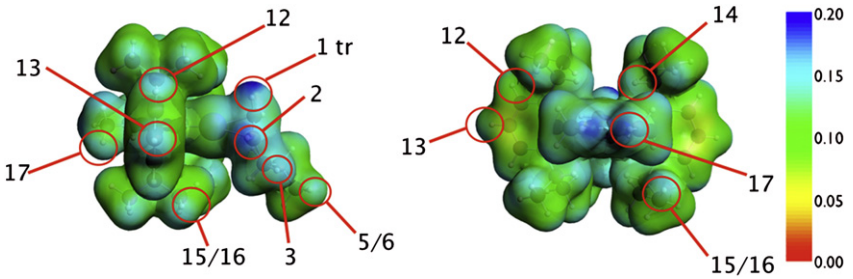

Fig. 5. Two views of the Coulomb potential of 2^+ mapped on an electronic isodensity surface ($\rho = 0.007$ e/Å^3, Coulomb potential in a.u.).

All manipulations of moisture-sensitive materials were performed in flamed Schlenk glassware on a Schlenk line, interfaced to a high vacuum pump, or in a nitrogen filled glove box. *n*-Pentane and CH_2Cl_2 were preventively distilled after 12 h of reflux over Na and CaH_2, respectively and freeze-pump-thaw degassed. CD_2Cl_2 was freeze-pump-thaw degassed over CaH_2 and vacuum transferred in storage Schlenk flasks with a PTFE valve.

4.1.1. Synthesis of complex ***1***BF_4

[1,3-Bis(di-iso-propylphenyl)imidazol-2-ylidene]Au–Cl (97 mg, 0.000160 mol) was charged in a Schlenk flask within a glove box. The Schlenk flask was interfaced with the high-vacuum line and about 5 mL of CH_2Cl_2 and 2.5 equiv of 4-methyl-1-pentene (49 μL) were added by a micrometric syringe. $AgBF_4$ (35 mg, 0.000184 mol) was added to the mixture that was strongly stirred; in a few minutes a white-grey solid (AgCl) settled to the bottom of the Schlenk. The suspension was filtered through a celite pad. The volume of the solution was reduced to about 2 mL and 3 mL of *n*-pentane was added. A white solid was formed. The solid was filtered, washed with *n*-pentane and dried under vacuum, giving **1**BF_4 as a white powder (90 mg, yield = 65%). Anal. Calc. for $C_{34}H_{51}AuBF_4N_2$: C, 52.93; H, 6.66; N, 3.63. Found: C, 53.0; H, 6.7; N, 3.5. NMR tube for analysis was prepared within the glove box adding the suitable amount of **1**BF_4 into a J-Young NMR tube. The J-Young NMR tube was interfaced to the high-vacuum line and approximately 0.7 mL of CD_2Cl_2 was added.

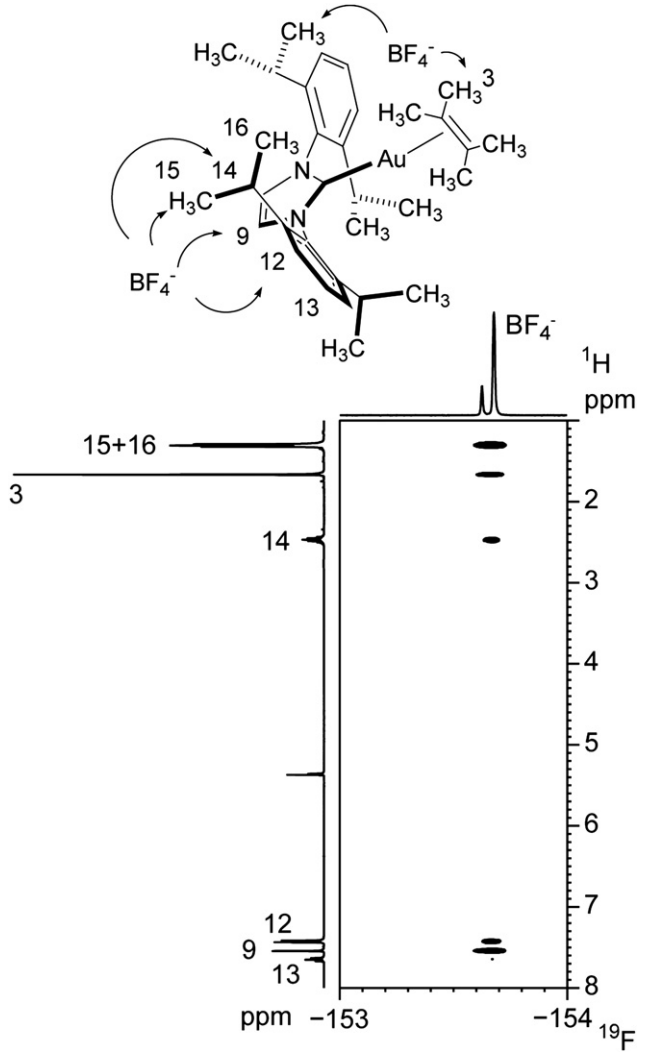

Fig. 6. $^{19}F,^1H$-HOESY NMR spectrum (376.65 MHz, 298 K, CD_2Cl_2) of complex **3**BF_4.

4.1.2. NMR data for ***1***BF_4

^1H NMR (CD_2Cl_2, 298 K, 400.13 MHz, *J* in Hz): δ 7.65 (d, $^3J_{13-12} = 7.9$, 13), 7.52 (s, 9), 7.40 (d, $^3J_{12-13} = 7.9$, 12), 5.36 (m, 2), 4.95 (d, $^3J_{1trans-2} = 8.8$, 1trans), 4.66 (d, $^3J_{1cis-2} = 17.0$, 1cis), 2.51 (sept, $^3J_{14-15} = {}^3J_{14-16} = 6.9$, 14), 1.70 (m, 3), 1.35 (m, 4), 1.30 (m, 15 and 16), 0.80 (d, $^3J_{5(6)-4} = 8.0$, 5 or 6), 0.75 (d, $^3J_{5(6)-4} = 8.0$, 5 or 6). $^{13}C\{^1H\}$ NMR (CD_2Cl_2, 298 K, 100.5 MHz, *J* in Hz): δ 180.8 (s, 8), 146.1 (s, 11), 133.8 (s, 2), 133.2 (s, 10), 131.9 (s, 13), 125.4 (s, 9), 125.0 (s, 12), 96.7 (s, 1), 44.5 (s, 3), 29.3 (s, 14), 25.0 (s, 15 or 16), 24.9 (s, 4), 24.1 (s, 15 or 16), 22.7 (s, 5 or 6), 21.4 (s, 5 or 6). ^{19}F NMR (CD_2Cl_2, 298 K): δ −153.35 (br, $^{10}BF_4$), −153.45 (br, $^{11}BF_4$).

4.1.3. Synthesis of complex ***2***BF_4

Complex **2**BF_4 was synthesized with the same procedure as **1**BF_4. Yield = 70%. Anal. Calc. for $C_{36}H_{55}AuBF_4N_2$: C, 54.07; H, 6.93; N, 3.50. Found: C, 54.3; H, 7.0; N, 3.4.

4.1.4. NMR data for ***2***BF_4

^1H NMR (CD_2Cl_2, 298 K, 400.13 MHz, *J* in Hz): δ 7.64 (d, $^3J_{13-12} = 7.9$, 13), 7.42 (d, $^3J_{12-13} = 7.9$, 12), 5.84 (m, 2), 4.88 (d, $^3J_{1tans-2} = 8.8$, 1trans), 4.66 (d, $^3J_{1cis-2} = 17.0$, 1cis), 2.40 (sept, $^3J_{14-15} = {}^3J_{14-16} = 6.9$, 14), 2.08 (s, 17), 1.80–1.55 (m, 3), 1.29 (m, 4, 15 and 16), 0.79 (d, $^3J_{5(6)-4} = 8.0$, 5 or 6), 0.74 (d, $^3J_{5(6)-4} = 8.0$, 5 or 6). $^{13}C\{^1H\}$ NMR (CD_2Cl_2, 298 K, 100.5 MHz, *J* in Hz): δ 177.2 (s, 8), 146.3 (s, 11), 132.5 (s, 2), 131.8 (s, 13), 131.6 (s, 10), 128.8 (s, 9), 125.2 (s, 12), 96.3 (s, 1), 44.4 (s, 3), 29.1 (s, 14), 25.5 (s, 4), 23.5 (s, 15 or 16), 24.1 (s, 15 or 16), 22.7 (s, 5 or 6), 21.5 (s, 5 or 6), 9.8 (s, 17). ^{19}F NMR (CD_2Cl_2, 298 K): δ −153.35 (br, $^{10}BF_4$), −153.45 (br, $^{11}BF_4$).

4.1.5. Synthesis of complex ***3***BF_4 *[17b]*

Complex **3**BF_4 was synthesized with the same procedure as **1**BF_4. Yield = 71%. Anal. Calc. for $C_{34}H_{51}AuBF_4N_2$: C, 52.93; H, 6.66; N, 3.63. Found: C, 53.0; H, 6.8; N, 3.5.

4.1.6. NMR data for ***3***BF_4

^1H NMR (CD_2Cl_2, 298 K, 400.13 MHz, *J* in Hz): δ 7.57 (d, $^3J_{13-12} = 7.9$, 13), 7.44 (s, 9), 7.31 (d, $^3J_{12-13} = 7.9$, 12), 2.40 (sept,

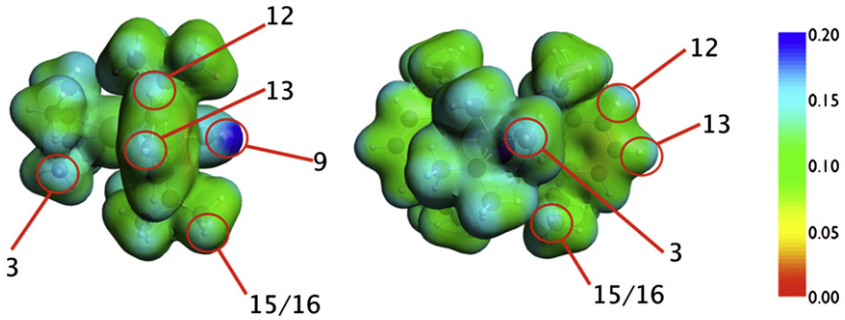

Fig. 7. Two views of the Coulomb potential of 3^+ mapped on an electronic isodensity surface ($\rho = 0.007$ e/Å^3, Coulomb potential in a.u.).

$^3J_{14-15} = {}^3J_{14-16} = 6.9$, 14), 1.60 (s, 3), 1.25 (m, 15 and 16). $^{13}C\{^1H\}$ NMR (CD_2Cl_2, 298 K, 100.5 MHz, *J* in Hz): δ 176.3 (s, 8), 145.7 (s, 11), 133.1 (s, 10), 131.4 (s, 13), 125.1 (s, 12), 124.4 (s, 9), 122.1 (s, 1) 28.8 (s, 14), 24.6 (s, 15 or 16), 24.0 (s, 15 or 16), 23.3 (s, 3). ^{19}F NMR (CD_2Cl_2, 298 K): δ −153.35 (br, $^{10}BF_4$), −153.45 (br, $^{11}BF_4$).

4.1.7. Synthesis of complex 4BF4 [21]

Complex **4**BF_4 was synthesized with the same procedure as **1**BF_4. Yield = 65%. Anal. Calc. for $C_{37}H_{49}AuBF_4N_2$: C, 55.17; H, 6.13; N, 3.48. Found: C, 55.3; H, 6.2; N, 3.4.

4.1.8. NMR data for 4BF4

^1H NMR (CD_2Cl_2, 298 K, 400.13 MHz, *J* in Hz): δ 7.61 (d, $^3J_{13-12} = 7.9$, 13), 7.47 (s, 9), 7.33 (d, $^3J_{12-13} = 7.9$, 12), 7.11 (d, $^3J_{5-4} = 8.3$, 5), 6.91 (d, $^3J_{4-5} = 8.3$, 4), 6.56 (dd, $^3J_{2-1cis} = 17.1$, $^3J_{2-1trans} = 9.6$, 2), 5.02 (d, $^3J_{1cis-2} = 17.1$, 1cis), 4.91 (d, $^3J_{1trans-2} = 9.6$, 1trans), 2.46 (s, 7), 2.40 (sept, $^3J_{14-15} = {}^3J_{14-16} = 6.9$, 14), 1.25 (d, $^3J_{15-14} = 6.9$, 15), 1.14 (d, $^3J_{16-14} = 6.9$, 16). $^{13}C\{^1H\}$ NMR (CD_2Cl_2, 298 K, 100.5 MHz, *J* in Hz): δ 179.84 (s, 8), 145.97 (s, 11), 144.30 (s, 3), 133.23 (s, 10), 131.43 (s, 13), 130.59 (s, 5), 129.90 (s, 6), 129.37 (s, 2) 128.13(s, 4), 125.20 (s, 9), 124.79 (s, 12), 84.73 (s, 1) 29.20 (s, 14), 24.74 (s, 16), 24.06 (s, 15), 21.62 (s, 7). ^{19}F NMR (CD_2Cl_2, 298 K): δ −153.35 (br, $^{10}BF_4$), −153.45 (br, $^{11}BF_4$).

4.2. NMR interionic characterization

4.2.1. NOE measurements

Two-dimensional $^{19}F,^1H$-HOESY NMR experiments were acquired using the standard four-pulse sequence [38]. The number of transients and data points were chosen according to the sample concentration and to the desired final digital resolution. Semi-quantitative spectra were acquired using a 1 s relaxation delay and 800 ms mixing times.

Table 4
Relative NOE intensities determined by arbitrarily fixing the intensities of the NOE(s) between the anion fluorines and the imidazolium protons 9 and 17 at 1 for **1**BF_4, **3**BF_4, **4**BF_4, and **2**BF_4, respectively.

	1BF_4	2BF_4	3BF_4	4BF_4 [21]
1trans	0.21	0.54	–	0.15
1cis			–	0.27
2	0.16	0.36	–	0.27
3	0.18	0.48	0.20	–
4	[a]	[a]	–	0.27
5	0.06	0.15	–	0.20
6			–	–
7	–	–	–	0.13
9	1.00	–	1.00	1.00
12	0.26	0.57	0.22	0.22
13	0.08	0.27	0.15	0.08
14	0.30	0.79	0.20	0.14
15	0.80	1.4	0.55	0.49
16				0.37
17	–	1.00	–	–

[a] Partially superimposed with protons 15 and 16.

4.3. Theoretical characterization of complexes

All calculations reported in this work were performed at the density functional theory (DFT) level using the ADF (Amsterdam Density functional) package [39,40]. The BLYP GGA functional was used [41]. The TZ2P triple zeta basis set with two polarization functions was used for all atoms. The relativistic effects were included with the ZORA [42] formalism as implemented in ADF. All the geometrical optimizations and the self consistent field (SCF) iterations have been performed including explicitly the using of the conductor like screening model (COSMO) as implemented in ADF [43]. The CH_2Cl_2 was used as solvent, with a dielectric constant of 8.93. A fine integration grid (the parameter of the numerical integration accuracy is 7) has been used both in the SCF iterations and in the optimization procedure, in order to converge properly the geometrical parameters.

Acknowledgements

This work was supported by grants from the Ministero dell'Istruzione, dell'Università e della Ricerca through PRIN 2007 (2007X2RLL2) and 2008 (2008KJX4SN 003) programs.

Appendix A. Supplementary information

Supplementary information associated with this article can be found in the online version, at doi:10.1016/j.jorganchem.2010.08.035.

References

[1] (a) B.H. Lipshutz, Y. Yamamoto, Chem. Rev. 108 (2008) 2793;
(b) G.J. Hutchings, M. Brust, H. Schmidbaur, Chem. Soc. Rev. 37 (2008) 1759.
[2] (a) A.S.K. Hasmi, Chem. Rev. 107 (2007) 3180;
(b) N. Bongers, N. Krause, Angew. Chem. Int. Ed. 47 (2008) 2178;
(c) Z. Li, C. Brouwer, C. He, Chem. Rev. 108 (2008) 3239;
(d) E. Jiménez-Nùnez, A.M. Echavarren, Chem. Rev. 108 (2008) 3326;
(e) D.J. Gorin, B.D. Sherry, F.D. Toste, Chem. Rev. 108 (2008) 3351;
(f) A. Arcadi, Chem. Rev. 108 (2008) 3266.
[3] (a) C. Brouwer, C. He, Angew. Chem. Int. Ed. 45 (2006) 1744;
(b) M. Schelwies, A.L. Dempwolff, F. Rominger, G. Helmchen, Angew. Chem. Int. Ed. 46 (2007) 5598.
[4] Z. Zhang, R.A. Widenhoefer, Org. Lett. 10 (2008) 2079.
[5] (a) M.A. Tarselli, A.R. Chianese, S.J. Lee, M.R. Gagnè, Angew. Chem. Int. Ed. 46 (2007) 6670;
(b) Y. Xia, A.S. Dudnik, V. Gevorgyan, Y. Li, J. Am. Chem. Soc. 130 (2008) 6940.
[6] J. Lacour, D. Linder, Science 317 (2007) 462.
[7] (a) G.L. Hamilton, E.J. Kang, M. Mba, F.D. Toste, Science 317 (2007) 496;
(b) R.L. LaLonde, B.D. Sherry, E.J. Kang, F.D. Toste, J. Am. Chem. Soc. 129 (2007) 2452.
[8] A.S.K. Hasmi, Nature 449 (2007) 292.

[9] A. Macchioni, Chem. Rev. 105 (2005) 2039 and references therein.
[10] A. Macchioni, Eur. J. Inorg. Chem. (2003) 195 and references therein.
[11] D. Zuccaccia, E. Foresti, S. Pettirossi, P. Sabatino, C. Zuccaccia, A. Macchioni, Organometallics 26 (2007) 6099.
[12] (a) D. Zuccaccia, G. Bellachioma, G. Cardaci, G. Ciancaleoni, C. Zuccaccia, E. Clot, A. Macchioni, Organometallics 26 (2007) 3930;
(b) A. Macchioni, A. Romani, C. Zuccaccia, G. Guglielmetti, C. Querci, Organometallics 22 (2003) 1526;
(c) D. Zuccaccia, G. Bellachioma, G. Cardaci, C. Zuccaccia, A. Macchioni, Dalton Trans. (2006) 1963;
(d) A. Macchioni, G. Bellachioma, G. Cardaci, G. Cruciani, E. Foresti, P. Sabatino, C. Zuccaccia, Organometallics 17 (1998) 5549.
[13] G. Bellachioma, G. Ciancaleoni, C. Zuccaccia, D. Zuccaccia, A. Macchioni, Coord. Chem. Rev. 252 (2008) 2224.
[14] (a) A. Correa, L. Cavallo, J. Am. Chem. Soc. 128 (2006) 10952;
(b) E. Clot, Eur. J. Inorg. Chem. (2009) 2319;
(c) A. Moreno, P.S. Pregosin, L.F. Veiros, A. Albinati, S. Rizzato, Chem. Eur. J. 15 (2009) 6848.
[15] (a) A.S.K. Hasmi, Angew. Chem. Int. Ed. (2010). doi:10.1002/anie.200907078;
(b) H. Schmidbaur, A. Schier, Organometallics 29 (2010) 2.
[16] (a) N.D. Shapiro, F.D. Toste, Proc. Natl. Acad. Sci U.S.A. 105 (2008) 2779;
(b) E. Herrero-Gómez, C. Nieto-Oberhuber, S. López, J. Benet-Buchholz, A.M. Echavarren, Angew. Chem. Int. Ed. 45 (2006) 5455;
(c) T.J. Brown, M.G. Dickens, R.A. Widenhoefer, Chem. Commun. (2009) 6451;
(d) T.N. Hooper, M. Green, J.E. McGrady, J.R. Patela, C.A. Russell, Chem. Commun. (2009) 3877;
(e) T.N. Hooper, M. Green, C.A. Russell, Chem. Commun. (2010) 2313.
[17] (a) N. Marion, S.P. Nolan, Chem. Soc. Rev. 37 (2008) 1776;
(b) T.J. Brown, M.G. Dickens, R.A. Widenhoefer, J. Am. Chem. Soc. 131 (2009) 6350;
(c) J.A. Akana, K.X. Bhattacharyya, P. Mueller, J.P. Sadighi, J. Am. Chem. Soc. 129 (2007) 7736;
(d) S. Flagge, A. Anoop, R. Goddard, W. Thiel, A. Furstner, Chem. Eur. J. 15 (2009) 8558;
(e) P. de Frémont, N. Marion, S.P. Nolan, J. Organomet. Chem. 694 (2009) 551.
[18] (a) V. Lavallo, G.D. Frey, S. Kousar, B. Donnadieu, G. Bertrand, Proc. Natl. Acad. Sci. U.S.A. 104 (2007) 13569;
(b) V. Lavallo, G.D. Frey, B. Donnadieu, M. Soleilhavoup, G. Bertrand, Angew. Chem., Int. Ed. 47 (2008) 5224.
[19] (a) M.A. Cinellu, G. Minghetti, F. Cocco, S. Stoccoro, A. Zucca, M. Manassero, M. Arca, Dalton Trans. (2006) 5703;
(b) D. Belli Dell'Amico, F. Calderazzo, R. Dantona, J. Straehle, H. Weiss, Organometallics 6 (1987) 1207;
(c) J.A. Flores, R.H.V. Dias, Inorg. Chem. 47 (2008) 4448.
[20] (a) J. Wu, P. Kroll, R.H.V. Dias, Inorg. Chem. 48 (2009) 423;
(b) R.H.V. Dias, J.A. Flores, J.A.J. Wu, P. Kroll, J. Am. Chem. Soc. 131 (2009) 11249;
(c) P. Schulte, U. Behrens, Chem. Commun. (1998) 1633.
[21] D. Zuccaccia, L. Belpassi, F. Tarantelli, A. Macchioni, J. Am. Chem. Soc. 131 (2009) 3170.
[22] D. Zuccaccia, L. Belpassi, L. Rocchigiani, F. Tarantelli, A. Macchioni, Inorg. Chem. 49 (2010) 3080.
[23] (a) G. Kovàcs, G. Ujaque, A. Lledòs, J. Am. Chem. Soc. 130 (2008) 853;
(b) C. Gourlaouen, N. Marion, S.P. Nolan, F. Maseras, Org. Lett. 11 (2009) 81;
(c) G. Kovàcs, G. Ujaque, A. Lledòs, Organometallics (2010). doi:10.1021/om100063v For a recent review on the theoretical chemistry of gold see:;
(d) P. Pyykkö, Chem. Soc. Rev. 37 (2008) 1967.
[24] (a) C. Zuccaccia, A. Macchioni, I. Orabona, F. Ruffo, Organometallics 18 (1999) 4367;
(b) A. Macchioni, A. Magistrato, I. Orabona, F. Ruffo, U. Rothlisberger, C. Zuccaccia, New J. Chem. 27 (2003) 455.
[25] G. Bellachioma, B. Binotti, G. Cardaci, C. Carfagna, A. Macchioni, S. Sabatini, C. Zuccaccia, Inorg. Chim. Acta 330 (2002) 44.
[26] D. Zuccaccia, A. Macchioni, Organometallics 24 (2005) 3476.
[27] B. Binotti, G. Bellachioma, G. Cardaci, C. Carfagna, D. Zuccaccia, A. Macchioni, Chem. Eur. J. 13 (2007) 1570.
[28] P. de Frémont, N.M. Scott, E.D. Stevens, S.P. Nolan, Organometallics 24 (2005) 2411.
[29] S. Gaillard, X. Bantreil, A.M.Z. Slawin, S.P. Nolan, Dalton (2009) 6967.
[30] E.J. Stoebenau III, R.F. Jordan, J. Am. Chem. Soc. 126 (2004) 11171.
[31] N. Salvi, L. Belpassi, F. Tarantelli, Chem. Eur. J. 16 (2010) 7231.
[32] L.N. Appelhans, D. Zuccaccia, A. Kovacevic, A.R. Chianese, J.R. Miecznikowski, A. Macchioni, E. Clot, O. Eisenstein, R.H. Crabtree, J. Am. Chem. Soc. 127 (2005) 16299.
[33] L. Busetto, M.C. Cassani, C. Femoni, A. Macchioni, R. Mazzoni, D. Zuccaccia, J. Organomet. Chem. 693 (2008) 2579.
[34] See for instance: (a) J. Mathew, C.H. Suresh, Inorg. Chem. 49 (2010) 4665.(b) P. Politzer, P. Lane, M.C. Concha, Y. Ma, J.S. Murray, J. Mol. Model. 13 (2007) 305;
(c) M. Alipour, A. Mohajeri, J. Phys. Chem. A (2010). doi:10.1021/jp104000c.
[35] S. Macura, R.R. Ernst, Mol. Phys. 41 (1980) 95.
[36] U.S. patent appl. 2006/7,109, 348, B1(2006), invs: S.P. Nolan.
[37] R. Uson, A. Laguna, M. Laguna, Inorg. Syn. 26 (1989) 85.
[38] B. Lix, F.D. Sönnichsen, B.D. Sykes, J. Magn. Reson. A 121 (1996) 83.
[39] G. te Velde, F.M. Bickelhaupt, S.J.A. van Gisbergen, C. Fonseca Guerra, E.J. Baerends, J.G. Snijders, T. Ziegler, J. Comput. Chem. 22 (2001) 931.
[40] ADF2008.01, SCM E.J. Baerends, J. Autschbach, A. Bérces, F.M. Bickelhaupt, C. Bo, P.M. Boerrigter, L. Cavallo, D.P. Chong, L. Deng, R.M. Dickson, D.E. Ellis, M. van Faassen, L. Fan, T.H. Fischer, C. Fonseca Guerra, S.J.A. van Gisbergen, A.W. Götz, J.A. Groeneveld, O.V. Gritsenko, M. Grüning, F.E. Harris, P. van den Hoek, C.R. Jacob, H. Jacobsen, L. Jensen, G. van Kessel, F. Kootstra, M.V. Krykunov, E. van Lenthe, D.A. McCormack, A. Michalak, J. Neugebauer, V.P. Nicu, V.P. Osinga, S. Patchkovskii, P.H.T. Philipsen, D. Post, C.C. Pye, W. Ravenek, J.I. Rodriguez, P. Ros, P.R.T. Schipper, G. Schreckenbach, J.G. Snijders, M. Solà, M. Swart, D. Swerhone, G. te Velde, P. Vernooijs, L. Versluis, L. Visscher, O. Visser, F. Wang, T.A. Wesolowski, E.M. van Wezenbeek, G. Wiesenekker, S.K. Wolff, T.K. Woo, A.L. Yakovlev, T. Ziegler, Theoretical Chemistry. http://www.scm.com.
[41] (a) A.D. Becke, Phys. Rev. A38 (1988) 3098;
(b) C. Lee, W. Yang, R.G. Parr, Phys. Rev. B. 37 (1988) 785.
[42] E. van Lenthe, A.E. Ehlers, E.J. Baerends, J. Chem. Phys. 110 (1999) 8943.
[43] C.C. Pye, T. Ziegler, Theor Chem Acc 101 (1999) 396.